Apoptosis and Overexpression of Bax Protein and *bax* mRNA in Smooth Muscle Cells Within Intimal Hyperplasia of Human Radial Arteries

Analysis With Arteriovenous Fistulas Used for Hemodialysis

Yukihiro Hayakawa, Genzou Takemura, Jun Misao, Motoo Kanoh, Michiya Ohno, Hiroshige Ohashi, Hisato Takatsu, Hiroyasu Ito, Kazunori Fukuda, Takako Fujiwara, Shinya Minatoguchi, Hisayoshi Fujiwara

Abstract—There is a type of arteriosclerosis with remodeling of middle-size arteries in which intimal hyperplasia of smooth muscle cells (SMCs) plays the main role, and there are few macrophages, T lymphocytes, and foam cells. It is unknown whether apoptosis and the expression of Bax, an inducer of apoptosis, are increased according to the progression of this type of human arteriosclerosis, which is different from so-called atherosclerosis. Bax heterodimerizes with Bcl-2, an inhibitor of apoptosis, and the ratio of Bax to Bcl-2 determines cellular apoptosis or survival. Thus, we investigated apoptosis and the expressions of Bax, *bax* mRNA, and Bcl-2 in human arteriovenous (AV) fistulas used for hemodialysis, a representative of arteriosclerosis of the aforementioned type. The material was 20 radial arteries obtained from 20 patients with chronic renal failure undergoing AV shunt surgery. SMCs, macrophages, and T lymphocytes were immunohistochemically identified at the light microscopic (LM) level. Apoptosis was detected by in situ terminal deoxynucleotidyl transferase (TdT)–mediated digoxigenin-dUTP nick end labeling (TUNEL) at both the LM and electron microscopic (EM) level. Cell proliferating activity was estimated by proliferating cell nuclear antigen (PCNA). Bax and Bcl-2 were detected by immunohistochemistry and Western blot analysis. Expression of *bax* mRNA was detected by in situ hybridization. LM TUNEL-positive cells in both the intima and media were significantly increased according to the percent stenosis of the vessels. EM analysis revealed that ultrastructures of apoptotic SMCs were seen in both synthetic and contractile phenotypes. Their frequency of occurrence in the intima and media were greater in those vessels with $>$50% stenosis than in those with $<$50% stenosis (5.2$\pm$0.7% versus 1.0$\pm$0.3% in the intima and 2.1$\pm$0.5% versus 0.2$\pm$0.1% in the media). The proportion of apoptotic SMCs with ruptured plasma membranes was greater than that of apoptotic SMCs with intact membranes in the intima of the former (4.1$\pm$0.6% versus 1.1$\pm$0.1%). Only those SMCs with apoptotic ultrastructures had TUNEL-positive nuclei with moderate or marked accumulation of immunogold particles at the EM level. However, ultrastructures of oncosis (primary necrosis) were not observed. Immunohistochemical analyses showed significant positive correlations between percent stenosis of vessels and the percentage of either PCNA-positive intimal cells or Bax-positive areas in the intima and media. Bcl-2–positive cells were not observed in the intima but mainly in the outer media. The percentage of Bcl-2–positive medial cells was definitely decreased at an early stage after formation of the AV fistula but did not change according to the duration of hemodialysis or the progression of arteriosclerosis. Western blot analysis of Bax or Bcl-2 and in situ hybridization of *bax* mRNA confirmed the immunohistochemical data. Thus, regulation of cellularity in intimal hyperplasia of SMCs in human arteriosclerosis with remodeling is mediated by proliferation and apoptosis but not oncosis. The apoptosis is probably induced by an increase in the Bax to Bcl-2 ratio. **(*Arterioscler Thromb Vasc Biol.* 1999;19:2066-2077.)**

Key Words: apoptosis ■ arteriosclerosis ■ smooth muscle cells ■ Bax

Arteriosclerosis of middle-size arteries is classified into 2 types,[1–4] which we will designate types A and B. Type A is an arteriosclerosis in which macrophages, T lymphocytes, lipid-rich foam cells, and lipid deposits play main roles (the so-called atherosclerosis).[1,2] It involves fatty streaks and plaques, which are frequently observed in coronary, carotid, and femoral arteries. In type B arteriosclerosis, invasion and proliferation of medial smooth muscle cells (SMCs) in the intima play the main roles, while the roles of macrophages, T lymphocytes, foam cells, and lipid deposits are strictly

Received April 14, 1998; revision accepted January 8, 1999.

From the Second Department of Internal Medicine (Y.H., G.T., J.M., M.K., M.O., H.O., H.T., H.I., K.F., S.M., H.F.), Gifu University School of Medicine, Gifu, and the Department of Food Science (T.F.), Kyoto Women's University, Kyoto, Japan.

Correspondence to Hisayoshi Fujiwara, MD, Second Department of Internal Medicine, Gifu University School of Medicine. 40 Tsukasa-Machi, Gifu 500-8705, Japan.

***Arterioscler Thromb Vasc Biol.* is available at http://www.atvbaha.org**

limited.[3,4] Restenosis after angioplasty, arterial grafts after coronary artery bypass graft surgery, and arteriovenous (AV) fistulas for hemodialysis belong to type B arteriosclerosis. It is well known that type B arteriosclerosis and vascular remodeling progress rapidly in radial arteries with an AV fistula for hemodialysis in patients with chronic renal failure.[4,5]

Apoptosis, or programmed cell death, differs from oncosis (primary necrosis) in terms of its ultrastructural and biochemical features, including cytoplasmic and nuclear condensation, subsequent formation of membrane-bound apoptotic bodies, and oligonucleosomal DNA degradation.[6,7] It has been established that in addition to its role in normal development,[8,9] apoptosis has an important role in the pathogenesis of a variety of diseases, including cancer, AIDS, heart disease, and neurological disorders.[10]

Many recent studies have indicated the presence of apoptosis[11–19] and the expression of various apoptosis-related factors such as p53,[11] Fas,[12] interleukin-1β–converting enzyme,[13] and caspase 3,[14] all inducers of apoptosis, or Bcl-2,[11,12] an inhibitor of apoptosis, in human arteriosclerotic lesions. All of these studies were performed in human type A arteriosclerosis with 1 exception, a report by Isner et al.[11] Isner et al showed an increase of in situ terminal deoxynucleotidyl transferase (TdT)–mediated digoxigenin-dUTP nick end labeling (TUNEL)–positive cells at the light microscopic (LM) level, expression of p53, and no expression of Bcl-2 in the intimal hyperplasia of SMCs in restenosis after angioplasty, a representative of type B arteriosclerosis, in patients undergoing directional atherectomy. However, typical ultrastructures of apoptotic SMCs were not shown in their study, as we have pointed out.[17] At present, electron microscopic (EM) evidence is necessary to define the presence of apoptosis because techniques such as DNA laddering and TUNEL, which are based on DNA fragmentation, may not reliably differentiate between apoptosis and oncosis.[20] Therefore, it is yet unknown whether apoptosis is accelerated together with the progression of type B arteriosclerosis. In addition, Bcl-2 heterodimerizes with Bax,[21,22] which is an inducer of apoptosis[21–24] and a primary response gene of p53,[23,24] and the ratio of Bax to Bcl-2 in a given cell determines cellular death or survival after an apoptotic stimulus.[21,22] At present, the levels of expression of Bax protein and *bax* mRNA are unknown in human type B arteriosclerosis.

Thus, to examine apoptosis and the expression of Bax protein, *bax* mRNA, and Bcl-2 protein in relation to the degree of type B arteriosclerosis, EM analysis combined with TUNEL, immunohistochemistry, Western blot analysis, and in situ hybridization (ISH) were performed on radial arteries retrieved from patients with chronic renal failure who were undergoing AV shunt operation. The advantageous point of this model is that it is possible to obtain human arterial tissues transmurally with various degrees of type B arteriosclerosis in ring form.

Methods

Patients and Tissue Preparation

Twenty specimens were obtained from the radial arteries of 20 patients with chronic renal failure who were undergoing AV shunt surgery for hemodialysis. Six specimens were retrieved from the radial arteries at the time of the initial surgery. In the other 14 patients, the original AV shunt had occlusive lesions, and repeated surgeries for a new AV shunt were performed. At the time of repeated surgery, 14 ring-form specimens were retrieved from radial arteries between the original AV shunt and the new AV shunt. The percent stenosis of these 14 radial arteries was variable, as shown in Table 1. The clinical characteristics of these patients are also listed in Table 1. Estimated duration of renal failure ranged from 2 months to 7 years, 4 months. Informed consent was obtained from each patient. The study was approved by the Ethics Committee on Human Research of Gifu University, Gifu, Japan.

TABLE 1. Clinical Characteristics of Patients

Patient No.	Age, y	Sex	DM	HTN	HL	Duration of HD	% Stenosis
1*	48	M	−	−	−	0	6
2*	38	F	−	−	−	0	9
3	53	M	−	−	+	3 mo	10
4	72	M	−	+	−	1 y, 2 mo	15
5	62	F	−	+	−	2 y, 9 mo	18
6*	72	F	+	+	−	0	22
7*	73	F	+	+	+	0	23
8*	80	M	+	−	−	0	25
9*	80	F	+	+	−	0	33
10	59	F	+	−	+	1 y, 11 mo	41
11	72	M	+	−	+	10 mo	56
12	63	M	+	+	−	1 y, 6 mo	58
13	47	F	−	+	−	10 mo	63
14	54	M	+	+	−	2 mo	72
15	41	F	−	+	−	1 y, 5 mo	84
16	54	F	+	+	+	4 mo	84
17	73	M	−	+	−	7 y, 4 mo	88
18	39	F	−	+	+	1 y, 3 mo	89
19	57	M	+	−	−	4 mo	90
20	78	F	+	+	−	6 mo	93

*Indicates cases of initial surgery.

DM indicates diabetes mellitus; HTN, hypertension; HL, hyperlipidemia. Duration of hemodialysis (HD) was estimated from the beginning of HD after the patient underwent the initial AV shunt surgery. Percent stenosis of the vessel was calculated as follows: intimal area/(intimal area+lumen area)×100.

Immediately after the specimens were removed in ring form, part of each specimen was fixed in 10% neutral buffered formalin for 24 hours at 4°C, embedded in paraffin, and cut into 4-μm sections. These were used for TUNEL and immunohistochemistry of Bax, Bcl-2, α-smooth muscle actin, macrophages, T lymphocytes, and proliferating cell nuclear antigen (PCNA), as well as for staining with hematoxylin-eosin (H-E), Masson's trichrome, and elastic van Gieson's stains. A portion of the transmural specimens was embedded in OCT compound (Miles), frozen in LN_2, and stored at −80°C. The frozen specimens were cut into 4-μm sections on a cryostat at −20°C for ISH. Other small, transmural specimens obtained from the 10 even-numbered patients in Table 1 (for random sampling) were used for EM analysis.

Quantitative Analysis of Vessel Diameter and Percent Stenosis of Vessels

With the use of a multipurpose color image processor (model LUZEX 3U, Nikon), 4-μm-thick preparations stained with elastic van Gieson's stain were enlarged on a high-resolution color television monitor at a magnification of ×10 to ×40, and the vessel diameter, surface area of the media, and percent stenosis of the vessels were analyzed.[25] The inner border of the intimal layer and the inner (internal elastic lamina) and outer borders of the media were traced, and the areas and circumferences encircled by the tracings

were calculated automatically. Vessel diameter (2r) was calculated from the circumference of the outer border of the media (C) to exclude artifactual deformities, as follows: $2r=C/\pi$.[26] The lumen area (L) was calculated as the area encircled by the inner border of the intimal layer. The intimal area (I) was calculated as the area encircled by the inner border of the media minus the lumen area. The surface area of the media was calculated as the area encircled by the outer border of the media minus the area encircled by the inner border of the media. The percent stenosis of vessels was calculated as follows: $I/(I+L)\times 100$.[25]

In all cases, these parameters were quantified independently by 2 morphologists who did not know from which patient the tissue sections had been procured. The interobserver variabilities were small for vessel diameter, lumen area, intimal area, and surface area of the media ($r=0.993$, 0.985, 0.989, and 0.988, respectively).

In Situ TUNEL at the LM Level

The in situ TUNEL method was performed on all specimens. After deparaffinization, staining was performed by following the directions of the in situ apoptosis detection kit using the TdT enzyme (Apop-Tag, Oncor). Commonly used procedures were also applied for color development with 3,3′-diaminobenzidine tetrahydrochloride (DAB, Sigma Chemical Co) and H_2O_2 for immunohistochemistry, and sections were counterstained with hematoxylin.

EM Analysis

Transmural specimens of radial arteries were cut into 5 to 7 small specimens consisting of 1-mm cubes and fixed with 2.5% glutaraldehyde (pH 7.3) in 0.1 mol/L phosphate buffer for 4 hours at 4°C. They were postfixed in 1% buffered OsO_4 for 1 hour, dehydrated through a graded series of ethanol, and embedded in Epon medium.

Semithin sections (0.9 μm) were cut with a glass knife and stained with toluidine blue. Then ultrathin sections (90 nm) of the areas of interest were cut with a diamond knife, collected on 300-mesh copper or nickel grids, and double-stained with uranyl acetate and lead citrate before examination in an EM (H-800, Hitachi). Ten tissue specimens of radial arteries were grouped as 5 arteries with mild arteriosclerosis (percent stenosis $<50\%$, mild sclerosis group) and 5 arteries with marked arteriosclerosis (percent stenosis $\geq 50\%$, marked sclerosis group).

The EM TUNEL analysis was performed on 10 specimens obtained from 10 patients by using the same method that we previously reported.[27] In brief, ultrathin sections (90 nm) were collected on bare 300-mesh nickel grids. The fragmented DNA was labeled on the thin sections by using components of the Apop-Tag kit. After the TdT enzymatic reaction was stopped, the grids were incubated with monoclonal mouse anti-digoxigenin antibody (0.4 μg/mL IgG, Boehringer Mannheim) for 30 minutes at room temperature. Next, they were incubated with 15-nm-gold–labeled goat anti-mouse IgG (Amersham) at a dilution of 1:50 in PBS for 1 hour at room temperature. They were then washed with PBS, rinsed in distilled water, counterstained with uranyl acetate and lead citrate, and examined in an EM. The grids were washed with PBS between steps. The validity of this method was checked by omitting TdT during the procedure as a negative control and by using prostate tissue from a rabbit castrated 2 days beforehand as a positive control.[28]

Immunohistochemical Procedures

The reactions were carried out using the indirect immunohistochemical technique. After deparaffinization, intrinsic peroxidase activity was inhibited by 0.3% H_2O_2 in methanol for 30 minutes, and nonspecific binding was blocked with normal goat serum. Primary antibodies for Bax (a polyclonal rabbit anti-human antibody, N-20, from Santa Cruz Biotechnology) or Bcl-2 (a monoclonal mouse anti-human antibody, 124, from DAKO A/S) were diluted 1:500 or 1:40, respectively, and incubated with the sections overnight at 4°C. A secondary antibody, a peroxidase-conjugated $F(ab')_2$ fragment of goat anti-rabbit IgG[H+L] for primary rabbit antibody or a peroxidase-conjugated $F(ab')_2$ fragment of goat anti-mouse IgG[H+L] for primary mouse antibody (Jackson Immunoresearch Laboratories), was incubated with the sections at a dilution of 1:500 for 40 minutes at room temperature. Sections were then stained with 0.4 mg/mL DAB and 0.006% H_2O_2 in 50 mmol/L Tris-HCl buffer (pH 7.4) for 5 minutes at room temperature. Between steps, the sections were washed with distilled water or PBS. Finally, the sections were counterstained with hematoxylin.

With the use of serial sections, cell types in the vessel wall were identified by immunohistochemistry. SMCs were stained by using a monoclonal antibody against human α-smooth muscle actin (1A4, DAKO A/S), and macrophages and T lymphocytes were identified by using monoclonal antibodies to human macrophages (PG-M1, DAKO A/S) and mature activated T lymphocytes (CD45RO, DAKO A/S), respectively.

For double immunohistochemistry, sections were stained first by TUNEL as described above. After incubation with DAB, they were washed with PBS. Sections were blocked with normal goat serum and incubated with the primary antibodies (against α-smooth muscle actin or macrophages). The APAAP kit (DAKO A/S) was used for the second immunohistochemical reaction. The sections were then visualized with fuchsin substrate (DAKO A/S).

In all cases, proliferation activity was evaluated by immunohistochemical analysis for PCNA. The primary antibody (PC10, DAKO A/S) was diluted 1:50 and incubated with the sections overnight at 4°C. Subsequent procedures were done according to the directions of the LSAB 2 kit (DAKO A/S). Sections were then stained with a DAB-H_2O_2 solution for 5 minutes at room temperature and counterstained with hematoxylin.

Specificity of the immunological reaction was controlled by replacing the primary antibody with a rabbit immunoglobulin fraction (DAKO A/S) or mouse IgG1 (DAKO A/S) (negative control test). The specificity of primary antibodies against Bax and Bcl-2 was also confirmed by preabsorbing the primary antibody with the corresponding synthetic antigens (preabsorption test). Positive controls were lymphocytes within the germinal center of autopsied human lymph nodes for Bax and cells within the mantle region, marginal zone, and interfollicular regions for Bcl-2.

The presence of immunoreactivity in the vessel wall was assessed by LM examination. Two trained observers who were unaware of the tissue data reviewed the sections; the immunoreactivities of TUNEL, PCNA, Bax, Bcl-2, α-smooth muscle actin, macrophages, and T lymphocytes were graded in each vessel on the basis of discussions between the 2 observers about the positivity or negativity of the immunohistochemical reactions when the judgment of positive or negative was difficult. The interobserver variabilities were small ($r=0.962$ in TUNEL, 0.992 in PCNA, 0.989 in Bax, and 0.983 in Bcl-2). The proportions of Bax- and Bcl-2–positive cells were quantified by dividing the number of positive cells by the total cell number ($\approx 2909\pm 215$ and 3698 ± 297 cells in the intima and media, respectively) on a high-resolution color television monitor at $\times 100$ to $\times 200$ magnification. The proportions of cells with TUNEL-positive or PCNA-positive nuclei were quantified by dividing the number of labeled nuclei by the total number of nuclei ($\approx 1998\pm 415$ and 2868 ± 558 cells in the intima and media, respectively) on a high-resolution color television monitor.

Western Blot Analysis

Assessment of Bax and Bcl-2 protein expression in 8 arterial specimens, which were selected by random sampling, was performed using a standard Western immunoblotting technique. These tissues were homogenized at 4°C in radioimmunoprecipitation assay buffer [50 mmol/L Tris-HCl (pH 7.5), 150 mmol/L NaCl, 1% NP-40, 0.5% sodium deoxycholate, 0.1% SDS, 0.02% NaN_3, 1 mmol/L PMSF, and 10 μmol/L leupeptin] and centrifuged. Protein concentrations of soluble fractions of tissue lysates were determined using Bio-Rad protein assay reagents (Bio-Rad Laboratories). Aliquots of 30 μg of total cellular protein were denatured by boiling with SDS and DTT, electrophoresed on 12.5% SDS-polyacrylamide gels, and then transferred to polyvinylidine difluoride membranes (Sequi-Blot PVDF membrane, Bio-Rad). After being blocked with 5% nonfat skim milk in TBS-T [10 mmol/L Tris-HCl (pH 7.5), 140 mmol/L NaCl, and 0.05% Tween 20] to block nonspecific binding overnight at 4°C, the membranes were probed by using either monoclonal anti-Bax or polyclonal anti–Bcl-2 antibodies, which were the same as those used for immunohistochemistry (1:1000 or 1:200 dilution, respectively,

with TBS-T containing 5% nonfat skim milk) for 1.5 hours. A secondary antibody, a peroxidase-conjugated $F(ab')_2$ fragment of goat anti-rabbit IgG[H+L] for the primary rabbit antibody or a peroxidase-conjugated $F(ab')_2$ fragment of goat anti-mouse IgG[H+L] for the primary mouse antibody, was incubated with the membranes at a dilution of 1:5000 for 1 hour at room temperature. Between steps, the membranes were washed with TBS-T. Finally, the membranes were developed using an enhanced chemiluminescence Western blotting determination kit (Amersham) and exposed to Kodak XAR-5 film (Eastman Kodak). Human lymph nodes obtained at lung surgery were used as positive controls for Bax and Bcl-2.

In Situ Hybridization

Total RNA of human lymph nodes obtained at lung surgery was isolated by the guanidinium thiocyanate–phenol-chloroform method[29] with the use of ISOGEN (Nippon Gene). To prepare human *bax* cDNA, we performed a reverse transcriptase–polymerase chain reaction (PCR) with human lymph node mRNA and synthesized oligonucleotide primers encoding human *bax*-α, 5′-GACCCGGTGCCTCAGGA-3′ (positions 142 through 158) and 5′-CCCCAGTTGAAGTTGCCGTCAG-3′ (positions 302 through 323). The sequences of PCR products were analyzed by the dideoxy chain-termination method and an ABI PRISM dye terminator cycle sequencing ready reaction kit (Perkin Elmer). A 182-bp *bax* cDNA fragment obtained by reverse transcriptase–PCR was subcloned into pGEM-T easy vector (Promega). The vector was linearized with *Nco*I for the SP6 promoter or *Spe*I for the T7 promoter. Digoxigenin-labeled riboprobes were transcribed with the DIG RNA labeling kit (SP6/T7, Boehringer Mannheim).

We checked the homology between the region of *bax* mRNA targeted by the probe and other members of the Bcl-2 family. The maximum percent homology of each Bcl-2 member compared with the region targeted by the *bax* probe was as follows; *bcl*-2 52.2%, *bcl*-xL 48.4%, *bcl*-xs 52.6%, *bcl*-xβ 27.4%, *bak* 52.0%, *mcl*-1 55.1%, *bad* 48.9%, *bcl*-w 20.0%, *a1* 54.5%, *bfl*-1 54.5%, BHRF-1 24.1%, E1B19K 51.3%, *bik* 51.9%, *bim* 46.9%, and *hrk* 41.2%. Although the targeted region of *bax* contained the Bcl-2 homology 2 domain, the maximum percent homology of each gene with the sequence of the region of the *bax* mRNA targeted by the *bax* probe was found to be <56%. Furthermore, we confirmed the specificity of the *bax* probe by Northern blot analysis by using a DIG nucleic acid detection kit (Boehringer) under the same conditions as used for ISH.

Cryosections were treated with paraformaldehyde, proteinase K, 0.2N HCl, and then acetic anhydride in triethanolamine. Fifty microliters of hybridization buffer (Hybrisol I containing 50% formamide, Oncor) containing the *bax* antisense cRNA probe was applied to each section, and the sections were hybridized for 16 hours at 50°C. Slides were then washed twice in 2× SSC with 50% formamide for 15 minutes and incubated with 20 μg/mL RNase A for 30 minutes at 37°C. Finally, after a high-stringency wash in 0.2× SSC for 15 minutes at 50°C, immunological detection of digoxigenin was performed with a DIG nucleic acid detection kit (Boehringer Mannheim). As negative controls, ISH with sense probes and RNase digestion of sections before hybridization were performed.

Statistical Analysis

Correlations between percent stenosis of the vessels and other parameters or between surface area of the media and vessel diameter were determined with simple linear regression and Pearson's correlation coefficient. Differences in the relationship between percent stenosis of vessels and other parameters were evaluated by ANCOVA. Bivariate analysis among percent stenosis of vessels, duration of hemodialysis, and other parameters was performed using multiple regression analysis. Quantitative data were expressed as mean±SEM. Differences between data from 2 groups were assessed by Student's *t* test. Statistical significance was set at a level of $P<0.05$.

Results

Vessel diameter and surface area of the media were correlated significantly and positively with percent stenosis of the vessels. This result indicates that intimal thickening, enlargement of vessel diameter, and hypertrophy of the media play important roles in remodeling of grafted radial arteries (Figure 1).

More than 99% of cells in the thickened intima and media showed positive α-smooth muscle actin immunoreactivity in each of the radial arteries, regardless of the degree of arteriosclerosis. The percentage of cells with positive macrophage immunoreactivity was 0.4±0.2% and of cells with T-lymphocyte immunoreactivity was 0.1±0.1%. Lipid-rich foam cells and lipid deposits were rarely observed.

Clinical data for the 20 patients are summarized in Table 1. There was no significant correlation between percent stenosis of vessels and age of the patients. There were also no significant differences in percent stenosis of vessels between males and females or between the presence and absence of hypertension, diabetes mellitus, or hyperlipidemia.

EM Analysis

EM analysis revealed that 97.5±0.2% of SMCs in the media had features of the contractile phenotype, whereas in the intima, 61.8±2.3% of SMCs had features of the synthetic phenotype (Figures 2 and 3).

Typical apoptotic SMCs were identified on the basis of cell shrinkage, homogeneous condensation of chromatin along the nuclear periphery, structurally preserved and easily recognized cytoplasmic organelles, and no disruption of the plasma membrane with or without nuclear fragments surrounded by membranes (apoptotic bodies[7]; Figures 4A and 4C). SMCs with oncosis were identified by the presence of dispersed chromatin, structurally altered cytoplasmic organelles with swelling, and a defect or disruption of the plasma membrane.[7,18] Meanwhile, SMCs with cellular shrinkage and apoptotic homogeneous chromatin condensation of the nucleus, despite the presence of a ruptured cell membrane, were also defined as apoptotic SMCs in the advanced stage of the process[7] (Figures 2C and 3C). Apoptosis with and without rupture of the cell membrane was observed in SMCs with both the synthetic and contractile phenotype (Figures 2B, 2C, 3B, and 3C).

The results of quantitative analysis of EM findings are listed in Table 2. Most cells in the intima and media showed features of SMCs in both the mild and marked sclerosis groups. The proportion of SMCs undergoing apoptosis in both the intima and media was significantly higher in the marked sclerosis group than in the mild sclerosis group (5.2±0.7% versus 1.0±0.3% in the intima and 2.1±0.5% versus 0.2±0.1% in the media). In intimas from the marked sclerosis group, the percentage of apoptotic SMCs with ruptured cell membranes was significantly higher than that of apoptotic SMCs with intact membranes (4.1±0.6% versus 1.1±0.1%). However, in medias from the marked sclerosis group and in both intimas and medias of the mild sclerosis group, differences between the proportion of apoptotic SMCs with ruptured cell membranes and apoptotic SMCs with intact membranes were not significant. SMCs with features of oncosis were not observed. There were a few macrophages, which were characterized by abundant lysosomes filled with remnants of phagocytosed cells and no myofilaments (Table 2). The percentage of macrophages in the intima was significantly higher in the marked sclerosis group than in the mild sclerosis group (0.3±0.1% versus 0.1±0.1%) However, these

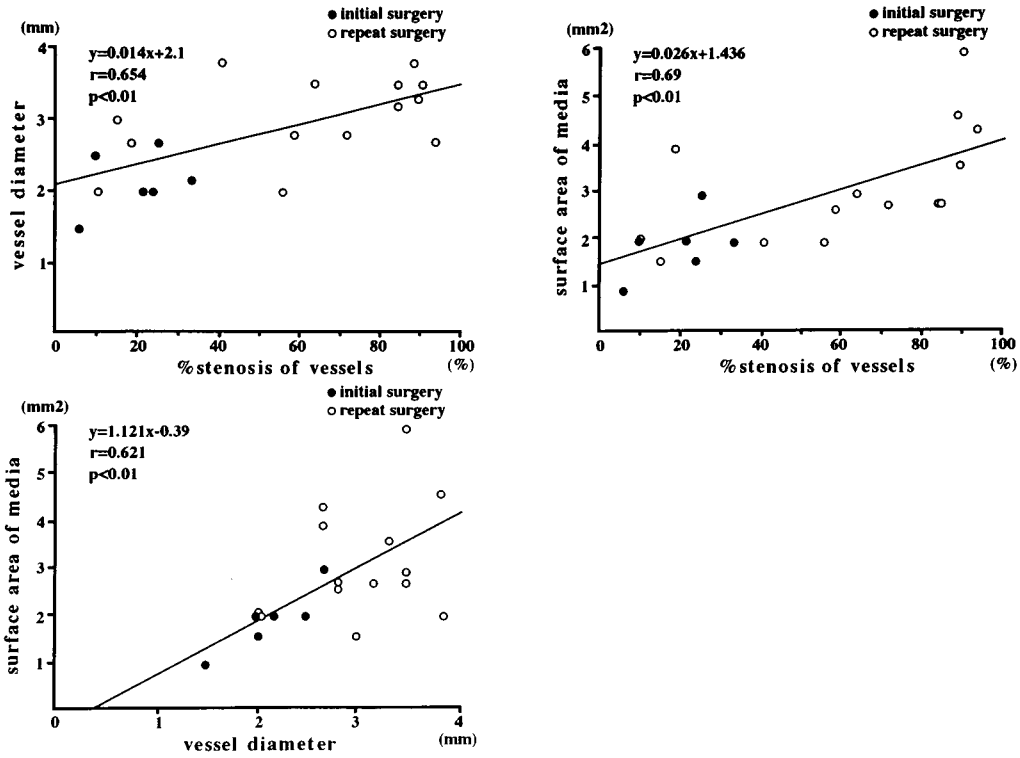

Figure 1. Correlations between percent stenosis of vessels and vessel diameter or surface area of media. Data show significant positive correlations between percent stenosis of vessels and vessel diameter or surface area of media and between surface area of media and vessel diameter (r=0.654, 0.690, and 0.621, respectively). This indicates that vessel diameter and surface area of the media were significantly increased (vascular remodeling) according to the progression of arteriosclerosis. ● Indicates arteries retrieved during initial surgery; ○, arteries retrieved during repeated surgery.

macrophages contained only a few cytoplasmic lipid droplets, and there was no evidence of exclusively lipid-loaded foam cells. There were also a few lymphocytes, which were characterized by small, rounded, and well-preserved cells with little cytoplasm and few organelles (Table 2). In the present study, most cells that had phagocytosed apoptotic SMCs were not macrophages but SMCs.

In EM TUNEL, the degree of accumulation of immunogold particles on normal-appearing SMCs was slight and limited to heterochromatin of the nuclei (Figure 4). However, EM TUNEL–positive nuclei with moderate to marked accumulations of immunogold particles, indicating DNA fragmentation, were observed only in apoptotic SMCs with and without ruptured cell membranes, and these features were similar to those of TUNEL-positive cells at the LM level (Figure 4). Accumulation of immunogold particles in the nuclei of apoptotic SMCs was limited to condensed chromatin.

In Situ TUNEL and PCNA

The proportion of cells with TUNEL-positive nuclei that had stained dark brown was correlated positively and significantly with percent stenosis of the vessels in both the intima and media (r=0.729 and 0.644, respectively, Figure 5). The heterogeneity of apoptotic activity of the sections was slight. The percentage of cells with PCNA-positive nuclei that had stained dark brown was correlated positively and significantly with percent stenosis of vessels in the intima (r=0.672). Double staining with anti–α-smooth muscle actin antibody and TUNEL or PCNA showed that these TUNEL- or PCNA-positive cells were SMCs (Figure 6).

Immunohistochemistry for Bax and Bcl-2

In the positive-control sections (lymph nodes), Bax immunoreactivity was observed in most cells within the germinal center. This was particularly intense in large cells, which were probably macrophages with a “starry sky” appearance. However, the majority of cells in the mantle region, marginal zone, or interfollicular region were negative (Figure 6B1). Conversely, Bcl-2 immunoreactivity was not observed in the germinal center but in the mantle region, marginal zone, and interfollicular region (Figure 6B2). These features were the same as descriptions in a previous report.[30] Serial sections of positive sections incubated with rabbit immunoglobulin fraction or mouse IgG1 showed no positive immunoreactivity (negative-control test). Immunostaining of those sections for Bax or Bcl-2 was completely inhibited by preabsorption of the primary antibody with the corresponding synthetic antigen (preabsorption test).

In arteries with mild sclerosis, few cells with Bax immunoreactivity were observed in the intima and inner media, but they were observed mainly in the outer media, as shown in Figure 6C3. In arteries with marked sclerosis, these cells were diffusely seen in both the intima (Figure 6D3) and media (Figure 6D6). Regression analysis showed significant positive correlations between percent stenosis of the vessels and Bax-positive percentages in the intima and media (r=0.827 and r=0.739, respectively, Figure 7). Cells with positive Bcl-2 immunoreactivity were not observed in the intima, but in the media, especially in its outer half (Figure 6). The percentage of Bcl-2–positive areas in the media was significantly decreased after formation of the AV fistula

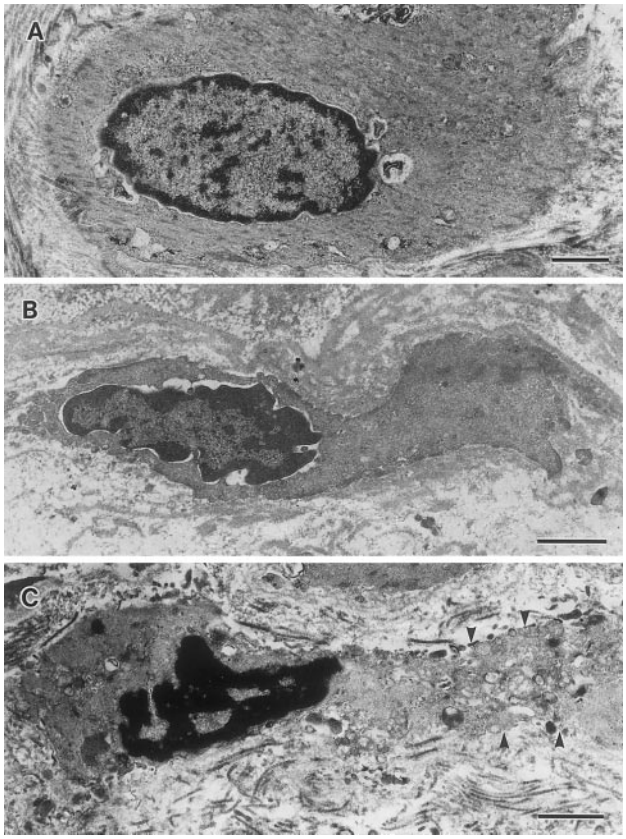

Figure 2. EM photomicrographs of normal-appearing and apoptotic SMCs with the contractile phenotype in radial arteries. A, Normal-appearing SMC with contractile phenotype. Note that cytoplasm is filled with abundant microfilaments with dense bodies while cytoplasmic organelles are rare. B, Apoptotic SMC without a ruptured plasma membrane. Marked and eccentric condensation of nuclear chromatin, wide perinuclear spaces, and cellular shrinkage are seen. Note that cytoplasm has features of the contractile phenotype shown in A. C, Advanced stage of apoptotic SMC with disruption of plasma membrane. Marked chromatin condensation and cellular shrinkage indicate that the SMC is apoptotic, despite membrane disruption (arrowheads) and dispersed cytoplasmic organelles in surrounding tissue. The cytoplasm also has features of the contractile phenotype shown in A. A, B, and C were obtained from tissue specimens of media from a radial artery with marked sclerosis. Bars=1 μm.

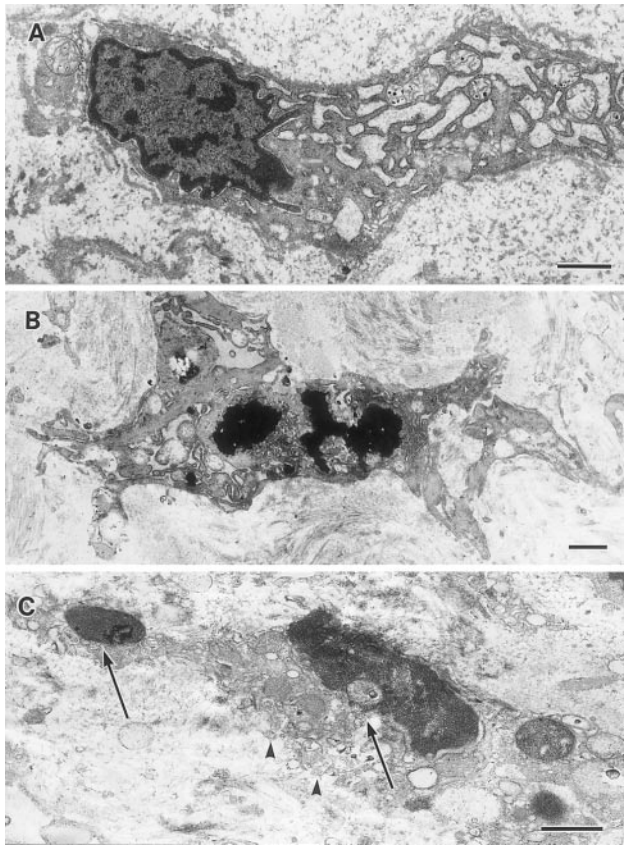

Figure 3. EM photomicrographs of normal-appearing and apoptotic SMCs with the synthetic phenotype in radial arteries. A, Normal-appearing SMC with synthetic phenotype. Note small amount of intracytoplasmic filaments in contrast with prominent endoplasmic reticulum, abundant Golgi complexes, and mitochondria. B, Apoptotic SMC with intact plasma membrane. Note nuclear fragmentation with marked chromatin condensation and cellular shrinkage. Cytoplasmic organelles are relatively preserved, and there was no obvious rupture of the cell membrane. Note that cytoplasm has features of the synthetic phenotype shown in A. C, Budding, apoptotic SMC with 2 separate, fragmented, and condensed nuclei (arrows) and cytoplasm being torn off immediately before forming apoptotic bodies. Disruption of cell membrane (arrowheads) and altered organelles are also shown. Note that cytoplasm has features of the synthetic phenotype shown in A. A, B, and C were obtained from tissue specimens of intima of radial arteries with marked sclerosis. Bars=1 μm.

(29.5±5.3% in the initial surgery group versus 5.9±1.7% in the repeated surgery group). There were no significant correlations between Bcl-2–positive percentage and percent stenosis of the vessels in either group or between the Bcl-2–positive percentage and duration of hemodialysis in the repeated surgery group (Figure 7).

Western Blot Analysis

As shown in Figure 8, Bax was detected as a band at 21 kDa and Bcl-2 as a band at 26 kDa in arterial specimens as well as in lymph nodes. Expression of Bax protein was weak in each of 4 radial arteries with mild arteriosclerosis (patients 1, 3, 7, and 8) but strong in each of 4 radial arteries with marked arteriosclerosis (patients 12, 15, 16, and 19). In contrast, expression of Bcl-2 was strong in 3 radial arteries retrieved during the initial surgery (patients 1, 7, and 8), but weak in 5 radial arteries retrieved during repeated surgery (patients 3, 12, 15, 16, and 19).

In Situ Hybridization

The hybridization signals of *bax* mRNA were distributed in a manner similar to that of immunoreactive Bax protein (Figure 6). In each radial artery with mild arteriosclerosis, mRNA signals of *bax* were very weak. However, in each radial artery with marked arteriosclerosis, intense, dark purple *bax* mRNA signals were diffusely distributed in the thickened intima and media, indicating that levels of *bax* mRNA were upregulated. None of the negative-control sections hybridized with the corresponding concentration of the sense cRNA probe showed positive staining. Thus, the ISH data were compatible with those of immunohistochemistry as well as with those of Western blot analysis.

Discussion

The present study revealed the following for human type B arteriosclerosis of radial arteries with AV fistulas used for hemodi-

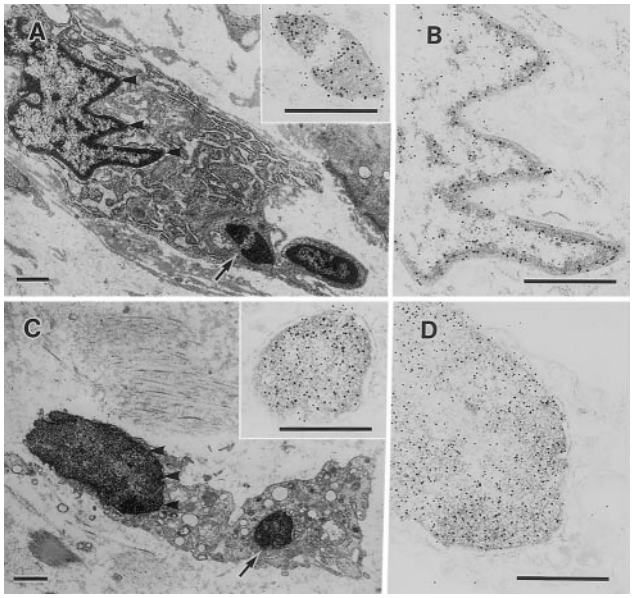

Figure 4. EM photomicrographs of SMCs stained with EM TUNEL method. In B and D, nuclei shown in A and C printed at normal contrast are presented at higher magnification and with higher contrast for clearer documentation of immunogold particles (small black dots). A, EM TUNEL of normal-appearing SMC with the synthetic phenotype, indicated by the small amount of intracytoplasmic filaments, prominent endoplasmic reticulum, and abundant Golgi complexes and mitochondria. Note phagocytosed apoptotic body from an adjacent apoptotic cell (arrow). Inset at upper right is the phagocytosed apoptotic body indicated by arrow in A, at higher magnification and higher contrast. Marked accumulation of immunogold particles are observed on the apoptotic body. B, Portion indicated by arrowheads in A at higher magnification and higher contrast. Note slight accumulation of immunogold particles on heterochromatin of nucleus. C, An SMC, presumably apoptotic/synthetic. Note marked condensation of chromatin and cellular shrinkage, suggesting apoptosis, findings similar to those for the synthetic phenotype shown in A. Note fragmented apoptotic body (arrow). Inset at upper right is the fragmented apoptotic body indicated by arrow in C, at higher magnification and higher contrast. Marked accumulation of immunogold particles are observed on the apoptotic body. D, Portion indicated by arrowheads in C at higher magnification and higher contrast. Note marked accumulation of immunogold particles on condensed nuclear chromatin, compared with that in B. Bars=1 μm.

alysis: (1) Apoptotic SMCs with typical ultrastructures of apoptosis and DNA fragmentation in both the intima and media were increased according to the progression of arteriosclerosis. (2) Expression of Bax protein and *bax* mRNA were also increased according to the progression of arteriosclerosis. (3) Bcl-2 expression in the intima was not seen in arteries with either mild or marked arteriosclerosis. Bcl-2 expression in the media was definitely decreased after formation of the AV fistula but did not change according to the progression of arteriosclerosis or the duration of hemodialysis.

Methodological Problems

Agarose gel electrophoresis of DNA is a popular and reliable method to detect DNA fragmentation as a biochemical marker of apoptosis, but it has a disadvantage in terms of low sensitivity.[31,32] In the present study, this method was not performed because the tissue specimens were too small to detect a DNA ladder. TUNEL at the LM level is useful for detection of DNA fragmentation in situ.[28,33] However, recent studies have shown that the DNA ladder and TUNEL are not specific markers for apoptosis and are also observed in cells with typical oncotic ultrastructures.[20] Therefore, we performed an EM analysis and EM TUNEL, in addition to LM TUNEL in the present study. The nuclear chromatin was slightly labeled with immunogold, suggesting DNA fragmentation, even in SMCs with normal-appearing ultrastructures, as shown in Figure 4B. Therefore, it is possible that a small amount of cleaved DNA was present even in normal SMCs or that slight cleavage of DNA occurred as an artifact during tissue processing. However, EM TUNEL–positive nuclei with moderate or marked accumulations of immunogold particles were observed only in ultrastructurally apoptotic SMCs, as shown in Figure 4D. Therefore, a moderate or marked accumulation of immunogold particles was considered indicative of apoptosis. The proportions of SMC apoptosis at the EM level were similar to those of TUNEL-positive cells at the LM level. Ultrastructures of oncosis were not observed in the present study. This suggests that most TUNEL-positive SMCs at the LM level are apoptotic.

Discrepancy exists in the literature concerning the expression of Bcl-2 in human medial SMCs.[11,12,34] For example, Isner et al[11] and the authors of the present study have reported positive immunoreactivity of Bcl-2, but Cai et al[12] and Kockx et al[34] reported negative immunoreactivity in human medial SMCs, although all studies showed the same result of no immunoreactivity in intimal SMCs. In addition, the specificity of some Bax antibodies has been questioned, because some of these show immunoreactivity in tissues of Bax-knockout mice. Therefore, the Bcl-2 and Bax antibodies used in the present study may have cross-reactivities between Bcl-2 and Bax. However, the present study showed that in the arterial wall of the repeated surgery group, Bcl-2 immunoreactivity was clearly decreased in medial SMCs compared with that of the initial surgery group and was not observed in intimal SMCs, despite definite overexpression of Bax immunoreactivity in both medial and intimal SMCs. In addition, we performed a Western blot analysis of Bcl-2 and Bax. Downregulation of Bcl-2 at 26 kDa, which was the predicted size for the *bcl*-2 gene, was seen in the repeated surgery group compared with the initial surgery group. Upregulation of Bax at 21 kDa, which was the predicted size for *bax* genes, was observed in radial arteries with marked arteriosclerosis compared with those with slight arteriosclerosis, as shown in Figure 8. The data confirmed the results of the immunohistochemical analyses. Thus, our data are considered to be independent of cross-reactivities of antibodies.

We examined whether the initial surgery data points were within the 95% CIs of the regression curve described by the repeated surgery data points. Each point in the former group was within the 95% CIs and did not significantly deviate from the regression curve with respect to vessel diameter, surface area of the media, and TUNEL-, PCNA-, or Bax-positive percentages. Furthermore, there were no significant differences between the initial surgery group and the repeated surgery group in these parameters by ANCOVA. A bivariate analysis was performed among percent stenosis of the vessels, duration of hemodialysis, and other parameters. This bivariate analysis showed that the duration of hemodialysis was not significantly correlated with these parameters. These find-

TABLE 2. Quantitative EM Analysis of Radial Arteries With Arteriosclerosis

		SMC						
	Total Cell No.	Normal, %	Apoptosis, %	Apoptosis Without RCM, %	Apoptosis With RCM, %	Oncosis, %	Macrophages, %	Lymphocytes, %
Intima								
Mild sclerosis group (n=5)	613±90	99.0±0.4*	1.0±0.3*	0.4±0.2*	0.6±0.2*	0	0.1±0.1*	0
Marked sclerosis group (n=5)	703±37	94.3±0.7*	5.2±0.7*	1.1±0.1*	4.1±0.6*	0	0.3±0.1*	0.2±0.1
Media								
Mild sclerosis group (n=5)	767±49	99.8±0.1	0.2±0.1*	0.1±0.1*	0.1±0.1*	0	0	0
Marked sclerosis group (n=5)	755±72	97.6±0.7	2.1±0.5*	0.9±0.3*	1.2±0.4*	0	0.2±0.2	0.1±0.1

Three randomly selected samples from each of 10 patient were examined. Total cell number is the summation of cells in the 3 tissue samples that were examined by EM. Mild sclerosis group had arteries with <50% stenosis. Marked sclerosis group had arteries with ≥50% stenosis.

RCM indicates rupture cell membrane.

*$P<0.05$.

ings indicate that for these parameters, analyses based on the percent stenosis of vessels and including patients undergoing initial and repeated surgeries are reasonable.

However, concerning the Bcl-2–positive portion of the media, 4 of 6 initial surgery data points were outside the 95% CIs, and there was a significant difference between the initial surgery group and the repeated surgery group by ANCOVA. These findings indicate that regression analysis based on percent stenosis of vessels and including patients undergoing initial and repeated surgeries may be inadequate for the Bcl-2–positive frequency. Therefore, correlations between percent stenosis of vessels and Bcl-2–positive frequencies were examined separately for each of the 2 groups. There was no significant correlation between percent stenosis of the vessels and Bcl-2–positive percentages in either group, indicating no change in Bcl-2 expression with respect to the progression of arteriosclerosis. Whereas the proportion of Bcl-2–positive cells was definitely decreased after formation of the AV fistula, it was similar for a long duration after that (Figure 7, lower right). Because the duration of hemodialysis was >2 months in all cases in the repeated surgery group, Bcl-2 in the media was downregulated at an early stage within 2 months after formation of AV the fistula, probably due to changes in blood flow.

Phenotypes of SMCs and Apoptosis, Bax Expression, or Bcl-2 Expression

EM analysis and immunohistochemical analysis with monoclonal anti–α-smooth muscle actin, anti-macrophage, and

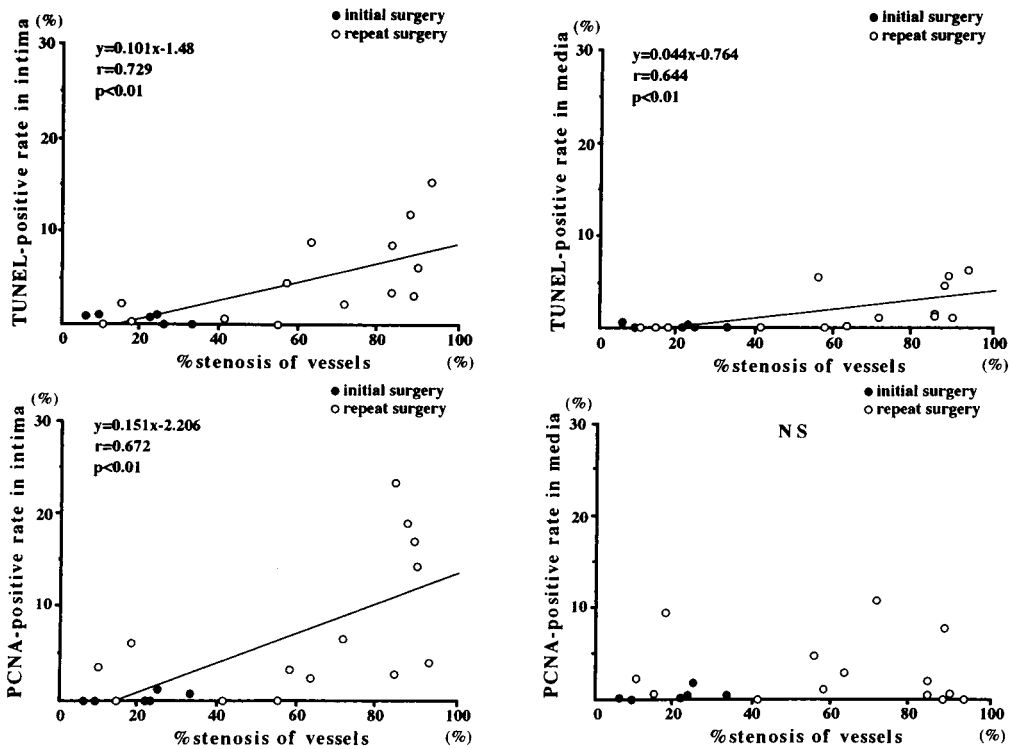

Figure 5. Correlation between percent stenosis of vessels and TUNEL- or PCNA-positive frequency. Data show significant positive correlations between percent stenosis of vessels and TUNEL-positive frequency in the intima and media or PCNA-positive frequency in the intima ($r=0.729$, 0.644, and 0.672, respectively). ● Indicates arteries retrieved during initial surgery; ○, arteries retrieved during repeated surgery.

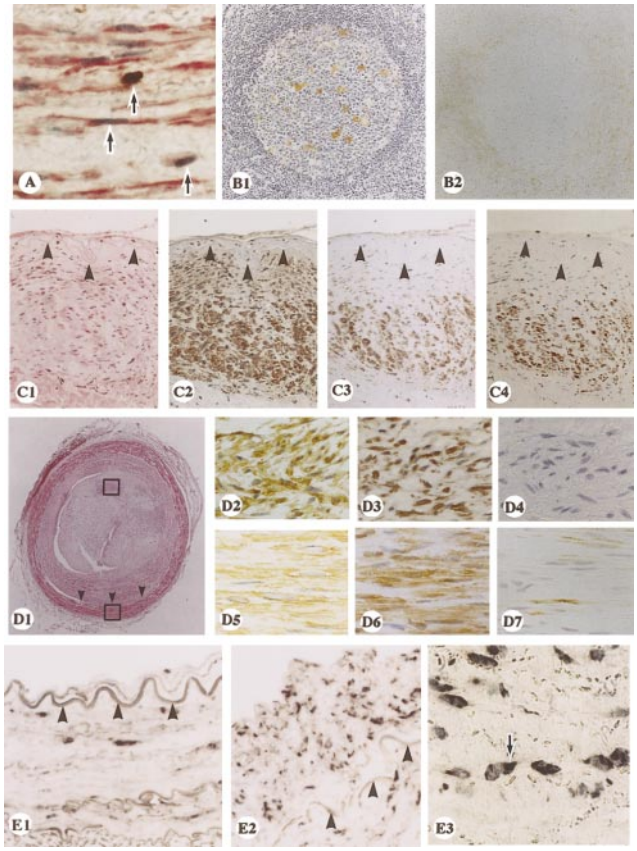

Figure 6. Immunohistochemical analysis and ISH of radial arteries. A, Double immunohistochemical staining with α-smooth muscle actin antibody and TUNEL in radial artery with marked arteriosclerosis. Note that cells indicated by arrows have positive α-smooth muscle actin immunoreactivity in the cytoplasm and brown TUNEL-positive nuclei. This indicates that TUNEL-positive cells are SMCs (original magnification ×400). Most SMCs show strong α-smooth muscle actin expression. However, apoptotic cells generally show decreases in differentiation markers. Immunoreactivity against α-smooth muscle actin was also considerably variable (from strong to weak) in TUNEL-positive cells in the present study. B1, Bax immunohistochemical staining of human lymph nodes as positive control. Bax immunoreactivity was observed in most cells within the germinal center. This was particularly intense in large cells, which were probably macrophages with a starry sky appearance. However, the majority of cells in mantle region, marginal zones, or interfollicular regions were negative (×40). B2, Bcl-2 immunohistochemical staining of human lymph nodes as positive control. Bcl-2 immunoreactivity was not observed in the germinal center but in mantle region, marginal zone, and interfollicular region (×40). In this specimen, counterstaining with hematoxylin to identify the nucleus was not done because of clear observation of positive Bcl-2 immunoreactivity in lymphocytes. Note that B1 and B2 are serial sections of the same tissue block. C1, H-E staining of radial artery obtained during initial surgery with mild sclerosis (patient 2) (×100). C2, α-Smooth muscle actin immunohistochemical staining of serial section in C1. Most cells in the media showed positive α-smooth muscle actin immunoreactivity (×100). C3, Bax immunohistochemical staining of serial section in C2 obtained from artery with mild sclerosis. Cells with dark brown positive immunoreactivity were seen mainly in the outer half of the media, but a few were seen in the intima. C3 and C4 are 2 serial sections. Same cells that are Bax-positive are considered to be also labeled for Bcl-2 (×100). C4, Bcl-2 immunohistochemical staining of serial section in C3 obtained from initial surgery group. Cells with dark brown positive immunoreactivity were seen mainly in the outer half of the media but were absent in the intima (×100). D1, H-E staining of radial artery obtained during repeated surgery with marked intimal thickening (patient 19). Upper square indicates portion of thickened intima. Lower square indicates portion of media (×15). D2, α-Smooth muscle actin immunohistochemical staining of upper square of D1. Most cells in thickened intima showed positive α-smooth muscle actin immunoreactivity, indicating that they were SMCs (×200). D3, Bax immunohistochemical staining of serial section in D2. Note that cells originating from SMCs in thickened intima show dark brown positive Bax immunoreactivity (×200). D4, Bcl-2 immunohistochemical staining of serial section in D3. Bcl-2 immunoreactivity was negative in SMCs in thickened intima (×200). D5, α-Smooth muscle actin immunohistochemical staining of lower square in D1. Most cells in the media showed positive α-smooth muscle actin immunoreactivity, indicating that they were SMCs (×200). D6, Bax immunohistochemical staining of serial section in D5. Note that most medial SMCs showed dark brown positive immunoreactivity (×200). D7, Bcl-2 immunohistochemical staining of serial section in D6 obtained from repeated surgery group. Cells with positive Bcl-2 immunoreactivity were seen in the media. However, they were fewer and had weaker immunoreactivity than did medial cells of initial surgery group shown in C4 (×200). E1, ISH of *bax* mRNA in radial artery with mild intimal thickening from initial-surgery group. Dark purple mRNA signals of *bax* were very weak in intima and media (×200). E2, ISH of *bax* mRNA in radial artery with marked intimal thickening from repeated surgery group. Intense dark purple *bax* mRNA signals were diffuse in the thickened intima and media (×200). E3, Higher-magnification view of E2 with hematoxylin nuclear staining. Note that specific hybridization signals of *bax* mRNA were mostly in perinuclear regions as indicated by arrow (×600). Black arrowheads indicate internal elastic lamina.

anti–T lymphocyte antibodies revealed that most cells in the intima and media originated from SMCs in the radial arteries with mild or marked arteriosclerosis. In addition, the present EM study showed that SMCs with the synthetic phenotype were predominant in the intima, whereas most SMCs in the media showed the contractile phenotype. This observation confirms previous reports.[35] The present EM analysis and double immunohistochemical staining procedures with TUNEL and the anti–α-smooth muscle actin antibody at the LM level showed that most cells with ultrastructures characteristic of apoptosis were SMCs in both the media and intima.

Cells with definite Bax expression were diffusely scattered in the intima as well as in the media of arteries with marked sclerosis. On the other hand, cells with Bcl-2 expression were not observed in the intima but were localized in the media. Medial Bcl-2 expression was definitely decreased at an early stage after formation of the AV fistula but did not change according to the duration of hemodialysis or the progression of arteriosclerosis. Thus, Bax is expressed similarly in SMCs with the synthetic and contractile phenotypes. In contrast, Bcl-2 is not expressed in SMCs with the synthetic phenotype but is expressed only in a portion of SMCs with the contractile phenotype. Bcl-2 may be downregulated along with the phenotypic modulation of SMCs from the contractile to the synthetic phenotype. However, downregulation of Bcl-2 expression in medial SMCs of the repeated surgery group cannot be explained by phenotypic modulation.

Apoptotic SMCs With and Without Ruptured Cell Membranes

Majno and Joris[7] proposed the concept that cell death can be classified as either apoptosis or oncosis (primary necrosis) and that both of these progress to secondary necrosis at the final stage, in which rupture of the cell membrane or structurally altered organelles, respectively, are observed The present data, in which apoptotic SMCs with and without

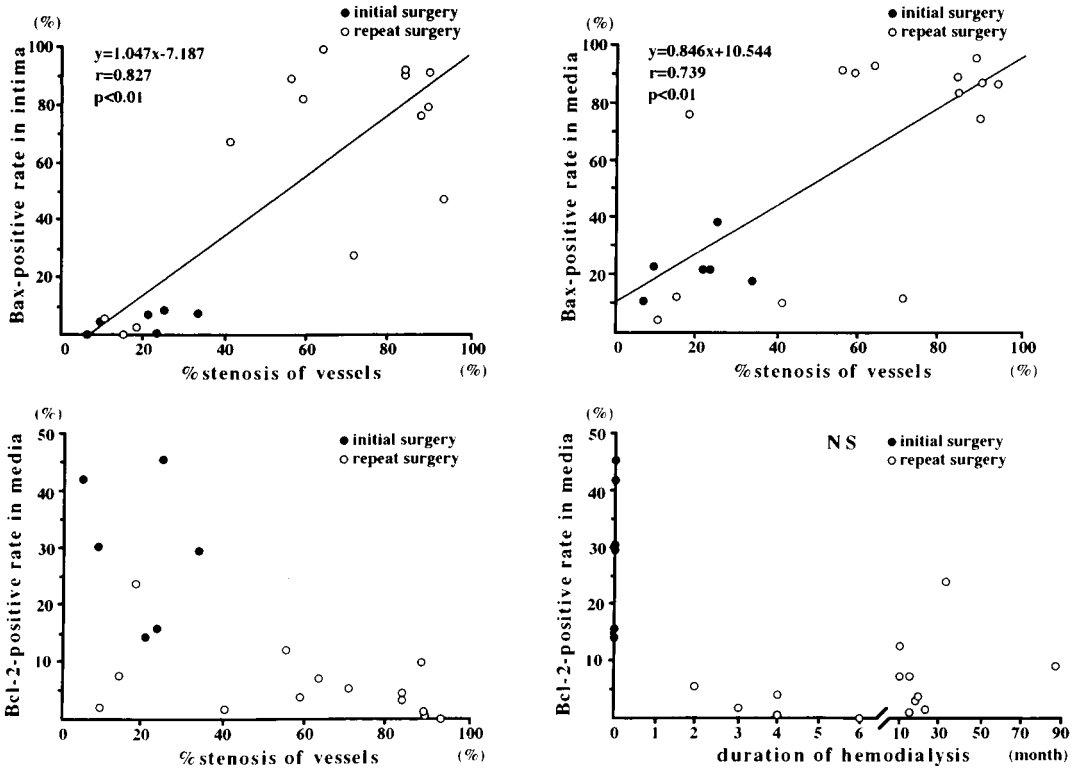

Figure 7. Correlation between percent stenosis of vessels and Bax- or Bcl-2–positive frequency and correlation between duration of hemodialysis and Bcl-2–positive frequency. Data show significant positive correlations between percent stenosis of vessels and Bax-positive frequency in the intima and media (r=0.827 and 0.739, respectively). In Bcl-2–positive frequency of the media, there was a significant difference between the initial surgery and repeated surgery groups by ANCOVA. Therefore, correlations between percent stenosis of vessels and Bcl-2–positive frequencies were examined in each group separately. There was no significant correlation between percent stenosis of vessels and Bcl-2–positive frequencies in either group. Percentage of Bcl-2–positive cells in the media was definitely decreased after formation of the AV fistula but was similar afterward (lower right panel). Note that duration of hemodialysis was >2 months in all cases in the repeated surgery group. ●, Arteries retrieved during initial surgery; ○, arteries retrieved during repeated surgery.

ruptured plasma membranes were observed, confirmed this concept. On the other hand, a recent study reported that although apoptosis clearly takes place in human type A arteriosclerosis, oncosis appears to be a much more common mechanism of cell death.[18] However, in the present study of type B arteriosclerosis, SMCs with oncosis were not observed. This fact suggests that apoptosis, but not oncosis, is a major mechanism of cell death in type B arteriosclerosis. This discrepancy may be explained by the histological and pathogenic differences between type A and type B arterioscleroses.

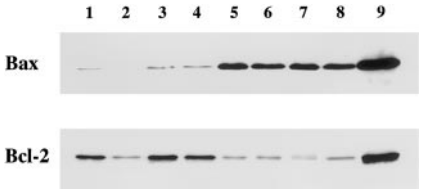

Figure 8. Western blot analysis of Bax and Bcl-2. Bax antibody detected a band at 21 kDa and Bcl-2 antibody detected a band at 26 kDa, which are predicted sizes for each gene product. Lane 1, patient 1; lane 2, patient 3; lane 3, patient 7; lane 4, patient 8; lane 5, patient 12; lane 6, patient 15; lane 7, patient 16; lane 8, patient 19 (Table 1); and lane 9, lymphocytes (positive control). Expression of Bax protein was very weak in radial arteries with slight arteriosclerosis (lanes 1 through 4). However, Bax protein levels were definitely elevated in radial arteries with marked arteriosclerosis (lanes 5 through 8). In contrast, data revealed a decrease in Bcl-2 protein in radial arteries from the repeated surgery group (patients 3, 12, 15, 16, and 19) compared with the initial surgery group (patients 1, 7, and 8).

It has been considered that apoptotic cell death usually does not result in release of intracellular contents and an ensuing inflammatory response, because apoptosis involves maintenance of membrane integrity and formation of apoptotic bodies, which are rapidly phagocytosed by adjacent cells.[7] In contrast, oncotic cell death occurs when cells swell and expel their contents into the extracellular environment, thereby eliciting an inflammatory response.[7] However, in the present study, EM analysis revealed that apoptotic cell death was frequently accompanied by cell membrane rupture, indicating release of intracellular contents into the extracellular environment. Nevertheless, inflammatory cell infiltration was strictly limited. Thus, in type B arteriosclerotic lesions of radial arteries, the noninflammatory mechanism of apoptotic cell death could not be explained by the lack of release of intracellular contents due to maintenance of membrane integrity and formation of apoptotic bodies. Some unknown mechanisms may exist in the apoptotic process that suppress an inflammatory response caused by the release of intracellular contents.

Pathophysiological Role of Apoptosis and Expressions of Bax and Bcl-2

Generally, normal tissue homeostasis is characterized by a balance between proliferation and apoptosis. A selective

increase of proliferation leads to hyperplasia, and a selective increase of apoptosis can result in atrophy and/or rarefaction. Hamet[36] proposed that remodeling represents a new balance between enhanced proliferation and apoptosis due to stimulation of both proliferation and apoptotic pathways. The above hypothesis was confirmed by the present study, because increases in PCNA-positive SMCs and apoptotic SMCs were observed in the thickened intima in concert with the progression of arteriosclerosis with remodeling. This suggests that induction of apoptosis secondary to the increase of proliferation may be protective against the progression of type B arteriosclerosis.

Bcl-2 as an antidote to apoptosis may be required to save progenitor and long-lived cells. Recently, a protective effect of Bcl-2 protein against apoptosis was shown in cultured vascular SMCs.[16] However, it has been reported that the *bcl*-2 gene family consists of >15 members that can be classified as antideath or prodeath. Bcl-2 is a prototype for an antideath, or survival, factor. Bax is a member of the Bcl-2 family, and when overexpressed, it can accelerate apoptotic death induced by cytokine deprivation in an interleukin-3–dependent cell line.[21] Overexpressed Bax also counters the death-repressor activity of Bcl-2.[21] That is, the ratio of Bax to Bcl-2 determines cellular death or survival after an apoptotic stimulus.[21,22] In the intimas examined in the present study, an increase in apoptotic cells and overexpression of Bax were observed according to the progression of arteriosclerosis, but expression of Bcl-2 was not observed. In the media, an increase in apoptotic cells and overexpression of Bax were also observed according to the progression of arteriosclerosis, but Bcl-2 expression was definitely decreased at an early stage after formation of the AV fistula but did not change according to the progression of arteriosclerosis. Thus, the ratio of Bax to Bcl-2 increased in the intima and media of markedly sclerotic arteries. Therefore, an increase of apoptosis in the intima and media in these arteries may be explained by an elevated ratio of Bax to Bcl-2, especially by overexpression of Bax. This finding is similar to that of type A arteriosclerosis described previously.[34]

Thus, we conclude that apoptosis and proliferation are accelerated and that Bax protein and *bax* mRNA are overexpressed in advanced human type B arteriosclerosis. Overexpression of Bax protein and *bax* mRNA may be important as a mechanism of SMC apoptosis. Understanding how SMC apoptosis is regulated by Bax protein may provide opportunities to develop new therapies for arteriosclerotic disease.

Acknowledgments

This study was supported in part by research grants 08457204 (H.F., 1996), 08670831 (T.F., 1996), 09470165 (H.F., 1997), 09670708 (G.T., 1997), and 09670707 (H.T., 1997) from the Ministry of Education, Science and Culture of Japan; the Japan Heart Foundation and Pfizer Pharmaceuticals Grant for Research on Coronary Artery Disease (Y.H., 1998). Thanks are given to Drs Emiko Ogawa and Yoshihiko Saito (Second Department of Internal Medicine, Kyoto University School of Medicine, Kyoto, Japan) for technical advice about ISH; Toshie Otsubo for assistance in preparing the manuscript; Yuki Shimomura, Noriko Ishida, Kaoru Kuroiwa, Tomoko Sugita, and Reiko Nitta for providing technical assistance; and Daniel Mrozek for reading the manuscript.

References

1. Stary HC, Chandler AB, Dinsmore RE, Fuster V, Glagov S, Insull W, Rosenfeld ME, Schwartz CJ, Wagner WD, Wissler RW. A definition of advanced types of atherosclerotic lesions and a histological classification of atherosclerosis. *Circulation*. 1995;92:1355–1374.
2. Ross R. The pathogenesis of atherosclerosis: a perspective for the 1990s. *Nature*. 1993;362:801–809.
3. Shelton M, Forman MB, Virmani R, Bajaj A, Stoney WS, Atkinson JB. A comparison of morphologic and angiographic findings in long-term internal mammary artery and saphenous vein bypass grafts. *J Am Coll Cardiol*. 1988;11:297–307.
4. Ejerblad S, Ericsson JLE, Eriksson I. Arterial lesions of the radial artery in uraemic patients. *Acta Chir Scand*. 1979;145:415–428.
5. Girerd X, London G, Boutouyrie P, Mourad JJ, Safar M, Laurent S. Remodeling of the radial artery in response to a chronic increase in shear stress. *Hypertension*. 1996;27:799–803.
6. Kerr JFR, Wyllie AH, Currie AR. Apoptosis: a basic biological phenomenon with wide-ranging implications in tissue kinetics. *Br J Cancer*. 1972;26:239–257.
7. Majno G, Joris I. Apoptosis, oncosis, and necrosis: an overview of cell death. *Am J Pathol*. 1995;146:3–15.
8. Cho A, Courtman DW, Langille BL. Apoptosis (programmed cell death) in arteries of the neonatal lamb. *Circ Res*. 1995;76:168–175.
9. Slomp J, Gittenberger de Groot AC, Glukhova MA, van Munsteren JC, Kockx MM, Schwartz SM, Koteliansky VE. Differentiation, dedifferentiation, and apoptosis of smooth muscle cells during the development of the human ductus arteriosus. *Arterioscler Thromb Vasc Biol*. 1997;17:1003–1009.
10. Thompson CB. Apoptosis in the pathogenesis and treatment of disease. *Science*. 1995;267:1456–1462.
11. Isner JM, Kearney M, Bortman S, Passeri J. Apoptosis in human atherosclerosis and restenosis. *Circulation*. 1995;91:2703–2711.
12. Cai W, Devaux B, Schaper W, Schaper J. The role of Fas/Apo 1 and apoptosis in the development of human atherosclerotic lesions. *Atherosclerosis*. 1997;131:177–186.
13. Geng YJ, Libby P. Evidence for apoptosis in advanced human atheroma: colocalization with interleukin-1β-converting enzyme. *Am J Pathol*. 1995;147:251–266.
14. Mallat Z, Ohan J, Leseche G, Tedgui A. Colocalization of CPP-32 with apoptotic cells in human atherosclerotic plaques. *Circulation*. 1997;96:424–428.
15. Björkerud S, Björkerud B. Apoptosis is abundant in human atherosclerotic lesions, especially in inflammatory cells (macrophages and T cells), and may contribute to the accumulation of gruel and plaque instability. *Am J Pathol*. 1996;149:367–380.
16. Bennett MR, Evan GI, Schwartz SM. Apoptosis of human vascular smooth muscle cells derived from normal vessels and coronary atherosclerotic plaques. *J Clin Invest*. 1995;95:2266–2274.
17. Takemura G, Hayakawa Y, Fujiwara H. Ultrastructure of apoptosis of smooth muscle cells. *Circulation*. 1996;94:1787–1788.
18. Crisby M, Kallin B, Thyberg J, Zhivotovsky B, Orrenius S, Kostulas V, Nilsson J. Cell death in human atherosclerotic plaques involves both oncosis and apoptosis. *Atherosclerosis*. 1997;130:17–27.
19. Hegyi L, Skepper JN, Cary NRB, Mitchinson MJ. Foam cell apoptosis and the development of the lipid core of human atherosclerosis. *J Pathol*. 1996;180:423–429.
20. Dong Z, Saikumar P, Weinberg JM, Venkatachalam MA. Internucleosomal DNA cleavage triggered by plasma membrane damage during necrotic cell death. *Am J Pathol*. 1997;151:1205–1213.
21. Oltvai ZN, Milliman CL, Korsmeyer SJ. Bcl-2 heterodimerizes in vivo with a conserved homolog, bax, that accelerates programmed cell death. *Cell*. 1993;74:609–619.
22. Hanada M, Aime-Sempec C, Sato T, Reed JC. Structure-function analysis of bcl-2 protein: identification of conserved domains important for homodimerization with bcl-2 and heterodimerization with bax. *J Biol Chem*. 1995;270:11962–11969.
23. Miyashita T, Reed JC. Tumor suppressor p53 is a direct transcriptional activator of the human bax gene. *Cell*. 1995;80:293–299.
24. Miyashita T, Krajewski S, Krajewska M, Wang HG, Lin HK, Liebermann DA, Hoffman B, Reed JC. Tumor suppressor p53 is a regulator of bcl-2 and bax gene expression in vitro and in vivo. *Oncogene*. 1994;9:1799–1805.
25. Tanaka M, Fujiwara H, Onodera T, Wu DJ, Matsuda M, Hamashima Y, Kawai C. Quantitative analysis of narrowings of intramyocardial small arteries in normal hearts, hypertensive hearts, and hearts with hypertrophic cardiomyopathy. *Circulation*. 1987;75:1130–1139.

26. Fujiwara T, Fujiwara H, Nakano H. Pathological features of coronary arteries in children with Kawasaki disease in which coronary arterial aneurysm was absent at autopsy: quantitative analysis. *Circulation*. 1988;78:345–350.
27. Takemura G, Ohno M, Hayakawa Y, Misao J, Kanoh M, Ohno A, Uno Y, Minatoguchi S, Fujiwara T, Fujiwara H. Role of apoptosis in the disappearance of infiltrated and proliferated interstitial cells after myocardial infarction. *Circ Res*. 1998;82:1130–1138.
28. Wijsman JH, Jonker RR, Keijzer R, van de Velde CJ, Cornelisse CJ, van Dierendonck JH. A new method to detect apoptosis in paraffin sections, in situ end-labeling of fragmented DNA. *J Histochem Cytochem*. 1993; 41:7–12.
29. Chomczynski P, Sacchi N. Single-step method of RNA isolation by acid guanidinium thiocyanate-phenol-chloroform extraction. *Anal Biochem*. 1987;162:156–160.
30. Krajewski S, Krajewska M, Shabaiki A, Miyashita T, Wang HG, Reed JC. Immunohistochemical determination of in vivo distribution of bax, a dominant inhibitor of bcl-2. *Am J Pathol*. 1994;145:1323–1336.
31. Rotello RJ, Hocker MB, Gerschenson LE. Biochemical evidence for programmed cell death in rabbit uterine epithelium. *Am J Pathol*. 1989; 134:491–495.
32. Desmouliere A, Redard M, Darby I, Gabbiani G. Apoptosis mediates the decrease in cellularity during the transition between granulation tissue and scar. *Am J Pathol*. 1995;146:56–66.
33. Gavrieli Y, Sherman Y, Ben-Sasson SA. Identification of programmed cell death in situ via specific labeling of DNA fragmentation. *J Cell Biol*. 1992;119:493–501.
34. Kockx MM, Meyer-Guido RY, Muhring J, Jacob W, Bult H, Herman AG. Apoptosis and related proteins in different stages of human atherosclerotic plaques. *Circulation*. 1998;97:2307–2315.
35. Thyberg J, Hedin U, Sjölund M, Palmberg L, Bottger BA. Regulation of differentiated properties and proliferation of arterial smooth muscle cells. *Arteriosclerosis*. 1990;10:966–989.
36. Hamet P. Proliferation and apoptosis of vascular smooth muscle in hypertension. *Curr Opin Nephrol Hypertens*. 1995;4:1–7.

Arteriosclerosis, Thrombosis, and Vascular Biology

JOURNAL OF THE AMERICAN HEART ASSOCIATION

Apoptosis and Overexpression of Bax Protein and *bax* mRNA in Smooth Muscle Cells Within Intimal Hyperplasia of Human Radial Arteries : Analysis With Arteriovenous Fistulas Used for Hemodialysis

Yukihiro Hayakawa, Genzou Takemura, Jun Misao, Motoo Kanoh, Michiya Ohno, Hiroshige Ohashi, Hisato Takatsu, Hiroyasu Ito, Kazunori Fukuda, Takako Fujiwara, Shinya Minatoguchi and Hisayoshi Fujiwara

Arterioscler Thromb Vasc Biol. 1999;19:2066-2077
doi: 10.1161/01.ATV.19.9.2066
Arteriosclerosis, Thrombosis, and Vascular Biology is published by the American Heart Association, 7272 Greenville Avenue, Dallas, TX 75231

Print ISSN: 1079-5642. Online ISSN: 1524-4636